Materials Research Proceedings 35 (2023) 191-197 https://doi.org/10.21741/9781644902714-23

Experimental analysis of FDM structures in shape memory polylactic acid

Maria Pia Desole[1,a], Annamaria Gisario[1,b*], Franco Maria Di Russo[1,c], Massimiliano Barletta[2,d]

[1] Sapienza Università di Roma, Dipartimento di Ingegneria Meccanica e Aerospaziale, Via Eudossiana 18, 001884 Roma (Italy)

[2] Università degli Studi Roma Tre, Dipartimento di Ingegneria Industriale, Elettronica e Meccanica, Via della Vasca Navale 79, 00146 Roma (Italy)

[a]mariapia.desole@uniroma1.it, [b]annamaria.gisario@uniroma1.it, [c]francomaria.dirusso@uniroma1.it, [d]massimiliano.barletta@uniroma3.it

Keywords: Additive Manufacturing, Energy Absorption, Shape Recovery

Abstract. The behavior of solid cellular structures in polylactic acid (PLA) manufactured by Fused Deposition Modeling (FDM) is herein investigated. In particular, the manuscript investigates the capability of permanently deformed PLA structures to restore their starting shapes, once a thermal stimulus is applied on them. In this study, a structure called Rototetrachiral was produced, which originates from Rotochiral and Tetrachiral. The latter was tested to verify its mechanical response and its ability to absorb energy when subjected to a compression stress, repeated over several cycles. The experimental results showed a close connection between the structure's ability to absorb energy and its extent of damage, which gradually increases with the number of cycles. Microscopic analysis shows that the central cells are the most deformed. However, the applied thermal stimulus allows to recover the deformation, ensuring good performance of the structure for a certain number of cycles.

1. Introduction

Shape memory materials are materials that once programmed into a temporary form, following an external stimulus, for example thermal, can return to their original configuration [1]. In the last decade, the applications in which they are involved are many: from the robotics sector [2], to the biomedical sector [3,4] and their presence is also evident in the civil engineering sector [5] and textiles [6,7]. Shape memory materials can be either polymeric [8], or metal alloys [9]. These materials combine well with the growing interest in additive technologies, in particular 4D printing [10,11]. 4D printing starts from the fundamentals of 3D printing, taking into account a fourth dimension, namely time [12,13]. By using additive technology and exploiting the properties of shape memory materials, we have seen how it is possible to study the behavior of certain types of reticular structures, for example chiral, anti-chiral, bio-inspired or auxetic [14]–[16]. Often such structures are studied from the mechanical point of view, but in reality they act as good energy absorbers, also thanks to the shape return properties of the material chosen for the manufacture. It has been seen in some studies as the design of the cell and the process parameters, influence in an important way the maximum compression load and energy absorption [17], [18]. PLA is more powerful than other polymers commonly used in FDM technology [19]. Changing printing parameters affects the compression behavior and the shape recovery of the cell structure. By varying the thickness of the layer, the printing speed, the temperature of the nozzle and the thermal stimulus of the product, it is clear that the latter is decisive for the trigger of the recovery of shape [20]. Until now, the reticular structures have been analysed, carrying out a single cycle of deformation-recovery of form, without further investigating what happens as the number of cycles

Materials Research Proceedings 35 (2023) 191-197 https://doi.org/10.21741/9781644902714-23

increases. In addition, there is no analysis of the state of damage to structures and how this affects the capacity of the structure to absorb energy. The following scientific paper analyses a chiral structure not present in the literature: the Rototetrachiral, inspired by the Tetrachiral and Rotochiral structures. These geometries were studied in [21]. Rototetrachiral has been designed as it has an intermediate absorption behaviour between Rotochiral and Tetrachiral. Wanting to carry out a series of cycles on the structure it was preferred to design a new structure with intermediate characteristics and with medium-high absorption capacity. Manufacturing was carried out using FDM additive technology and PLA was chosen as the material. Once it has been subjected to compression, its shape has been recovered by external thermal stimulus. The procedure was repeated over several cycles in order to assess the energy absorption capacity of the geometry. By means of a microscope visual analysis, it was analysed how the state of damage affects the mechanical properties of the structure, as well as the energy absorption of the structure.

2. Materials and Methods

2.1 Definition of geometry and material

The Rototetrachiral is a structure that has 4 adjacencies, that is 4 elements called arms, that originate from the circular element, arranged at 90°. The relative density chosen at the design stage is 0.153, lower than the geometries referred to. The pattern was then recreated in the CAD environment through the software "Autodesk Inventor 2021". Figure 1 shows the CAD model of the geometry (a), a front section of the geometry (b) and a detail of the cell (c).

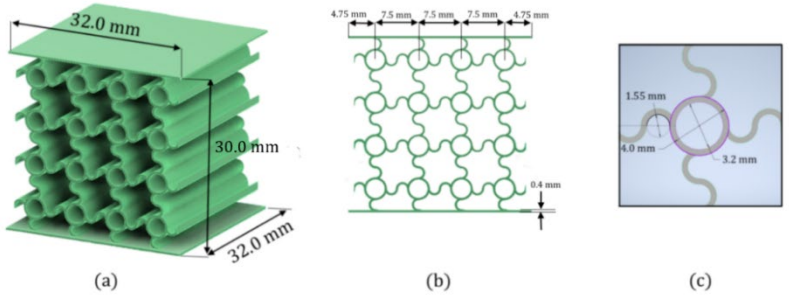

Figure 1. CAD model of the geometry (a), front section (b) and a detail of the cell (c).

ùThe 30x30x30 mm^3 cube is delimited by two layers (top and bottom respectively) of 4 mm thickness and 32x32 mm^2 dimension. The geometry was produced in PLA with green color. The 1 mm increase in layer size facilitates the increase of the adhesion surface with the plates and a more gradual stress distribution.

2.2 3D printing process

The production of the samples was done using FDM technology, with an Ultimaker 3D printer, model S5. The Software "Ultimaker Care" allowed you to set the print parameters.

In particular, attention was paid to the thickness of the layer and the printing speed of 0.2 mm and 50 mm/s, respectively chosen to obtain aesthetically appreciable products and not to induce states of residual stress [22]. The printing temperature was set to 200 ºC as per material datasheet, while the filling density of 100% was chosen to exhibit maximum mechanical strength. These parameters made sure to have three specimens dimensionally identical in height equal to 32 mm. The step of 1 mm in both the top and bottom layer is used to correctly realize the geometry, without problems of thermal expansion of the layers in contact with the plane. In this regard, a hydrophilic support in polyvinyl alcohol is inserted, removed as a result of the printing process.

Materials Research Proceedings 35 (2023) 191-197 https://doi.org/10.21741/9781644902714-23

2.3 Compression tests

Downstream of the production of the specimens they are subjected to the compression test, with the load applied perpendicular to the two layers. The machine used for the test is Shimadzu, model "Autograph AGS-X series" with 5 kN load cell and guaranteed maximum error of 1%. The standard considered for the test is the ASTM C365, specific to test compression sandwich structures made of polymer. The tests were carried out with a maximum displacement of 8 mm and the prescribed lowering speed of the plate of 3 mm/min. To ensure a certain reliability of the results and in the mechanical behaviour of the geometry, three replicates are made.

2.4 Springback and shape recovery

Springback is measured by means of a slide gauge, with measurements being taken for one hour every 5 minutes. For the recovery of form, on the other hand, the specimens are immersed in a bath at a controlled temperature of 75 ºC, higher than the glass transition of polylactic acid, which is about 62 ºC. A tracking software has been used to monitor the recovery of shape. Two markers are placed at the ends of the top layer and the movement has been traced, through the acquisition of recordings made with full HD JVC camera, model GZ-E205.

2.5 Cycle analysis and subsequent shape recovery

The above steps from the compression test to the shape return have been repeated for a total of 6 cycles. At the sixth cycle the structure suffered a permanent failure, to be no longer usable, so it was decided to finish the trial at the sixth cycle, leaving out the springback and form recovery phases for the sixth cycle.

3. Results and discussion

3.1 Compression tests 8 mm – 1st cycle

Figure 2a shows the Force-Displacement diagram of the 8 mm displacement compression test. From the graph you can see how the maximum load is reached near the displacement of 2 mm and is repeated, in a similar way for movements close to 4 and 6 mm. There are three peaks whose ascending phases correspond to the longitudinal deformation of the rows of cells that make up the sample. The first peak refers to the deformation of the central files, while the other two refer to the external files in contact with the layers. The descending phases instead correspond to the collapse of the row of cells.

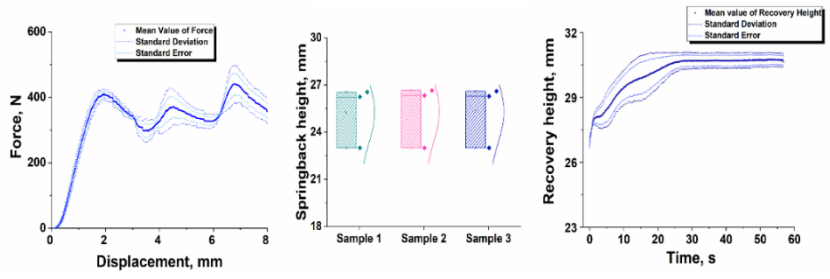

Figure 2. Force-Displacement diagram of the compression test at 8 mm (a), springback for the three samples (b) and the shape recovery (c)

The maximum load borne by the structure is slightly higher than 400 N, lower than other chiral structures, due to its low relative density [23].

Materials Research Proceedings 35 (2023) 191-197 https://doi.org/10.21741/9781644902714-23

3.2 Springback and shape recovery

For springback at zero time, the height value at the end of compression is considered. While at time t = 1 min, this refers to the height value at the instant after the plate separation. The springback height undergoes minimal variation in the three test pieces, with an average value of approximately 26 mm, indicating good replicability of the tests, as shown in Figure 2b. Figure 2c shows the average Rototetrachiral shape recovery model, measured over a time interval of 60 s. Recovery ends at 25 s and is not instantaneous due to geometric damage.

3.3 Compression tests 8 mm - up to the 6th cycles

Once a complete test cycle has been carried out, the following cycles have been carried out, until the geometry has been completely broken. Figure 3a shows the average trend of the Force-Displacement curves of the compression test for the 6 cycles envisaged. The graph shows that there is a strong load drop between the first and the second cycle, with the maximum load being reduced by about 38%. Between the second and third cycles, however, there is an almost overlap of the Force-Displacement curves and a limited load drop. A justification for this phenomenon can be found in the fact that the second and third cycles are carried out 48 hours apart, resulting in aging of the material. Similarly, the situation is repeated between the fifth and sixth cycles.

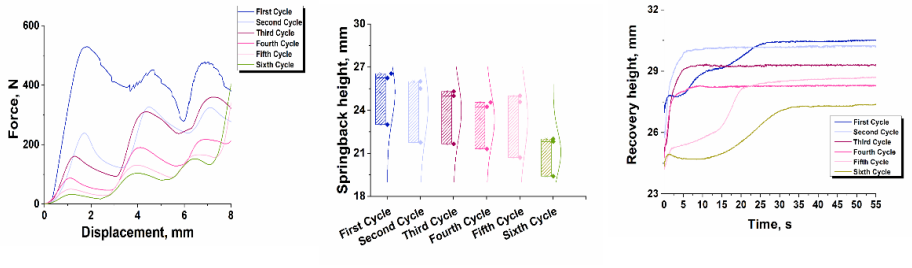

(a) (b) (c)

Figure 3. Force-Displacement diagram of the compression test up to the 6th cycles (a), springback for 6 cycles (b) and shape recovery for 6 cycles (c)

3.4 Springback and shape recovery for 6 cycles

Figure 3b shows the trend of springback that in the last cycle, unlike the first, is contained. The reduction of the average springback height between first and last cycles is greater than 5 mm and is due to increased mobility in the links between arms and circumferences, caused by repeated deformations. In the sixth cycle the structure is highly compromised, which justifies the limited springback. Figure 3c shows the recovery height average trend, highlighting how in the last cycles the recovery is slower, always because of the high damage of the structure.

3.5 Energy Absorption

The absorption energy is calculated using the Specific Energy Absorption (SEA) parameter, which normalizes the absorption energy measured from the subtended area of the Force-Displacement curve to the densification condition, relative to the mass of the structure [24].

Figure 4a shows the histogram describing the trend of normalized energy as cycles change. It is noted that in the first cycles the structure has a good level of energy absorption, averaging between 1180 mJ/g and 729 mJ/g. Absorption in the last three cycles amounts to an average value of 441 mJ/g, 340 mJ/g and 298 mJ/g respectively, with a significant decrease due to increased damage. There is no net change between the second and third cycles for the reasons described above. In the last cycle, despite the obvious fractures and injuries present in the structure, the level

of energy absorption does not decrease significantly. Therefore, it can be shown that the structure is a good energy absorber, even in the presence of permanent damage. Figure 4b shows the trend of the maximum peak as cycles change. In this case, the maximum load decreases, except between the second and third cycles and between the fifth and sixth, due to the aging of the material. As for the absorption in the last two cycles, there is a low decrease in the maximum load which is equal to an average value of about 154 N.

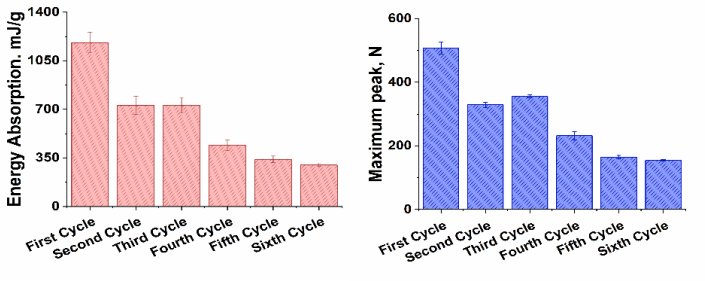

Figure 4. Energy absorption for 6 cycles (a) and maximum peak (b)

3.6 Microscopic analysis

Figure 5 shows the microscopic analysis of the structure after the first and sixth cycles.

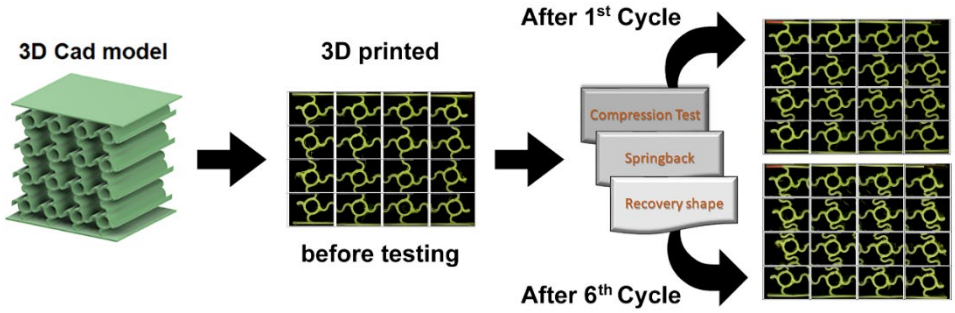

Figure 5. Microscopic analysis of the structure after the first and sixth cycles

Compared to the non-deformed configuration, the geometry is more damaged in the central region, particularly at the connection level between arms and circumferences.

4. Conclusions

In this paper, the behaviour of the Rototetrachiral cell structure has been evaluated, both mechanically and in terms of absorbed energy. The geometry was subjected to a static compression load and subsequent recovery of the shape repeated for six cycles. After the compression tests, the springback height was analysed and then the recovery of the specimen shape. The deformations induced by the subsequent compressive stresses can lead to a reduction in mechanical strength, albeit not substantially. The analysis shows that the geometry gives the structure a good ability to act as an energy absorber, particularly in the first cycles, when the sustainable load from the specimen is high. As number of cycles increase, absorption energy is reduced, with a decrease that can be estimated at 70% after the sixth cycle. For springback seems to be a correlation between damage and recovered height, with a decrease in height recovered elastically between first and sixth upper cycle of 16%. The same considerations can be extended to the recovery of shape.

Microscopic analysis shows that the central cells are the most damaged, while in the peripheral cells the arms connected respectively to the top and to the bottom layer do not show lesions. The application of a thermal stimulus shows how the deformation can be recovered, partly restoring the bonds within the structure and also affecting the mechanical performance of the same. Finally,

the adoption of three replicates was sufficient as the variability on the tests was found to be low and estimated to be less than 7%.

References

[1] A. Melocchi *et al.*, «Shape memory materials and 4D printing in pharmaceutics», *Adv. Drug Deliv. Rev.*, vol. 173, pp. 216–237, giu. 2021. https://doi.org/10.1016/j.addr.2021.03.013

[2] Xiaonan Huang, M. Ford, Z. J. Patterson, M. Zarepoor, C. Pan, e C. Majidi, «Shape memory materials for electrically-powered soft machines», *J. Mater. Chem. B*, vol. 8, fasc. 21, pp. 4539–4551, giu. 2020. https://doi.org/10.1039/D0TB00392A

[3] N. Sabahi, W. Chen, C.-H. Wang, J. J. Kruzic, e X. Li, «A Review on Additive Manufacturing of Shape-Memory Materials for Biomedical Applications», *JOM*, vol. 72, fasc. 3, pp. 1229–1253, mar. 2020. https://doi.org/10.1007/s11837-020-04013-x

[4] R. Sarvari *et al.*, «Shape-memory materials and their clinical applications», *Int. J. Polym. Mater. Polym. Biomater.*, vol. 71, fasc. 5, pp. 315–335, mar. 2022. https://doi.org/10.1080/00914037.2020.1833010

[5] I. Abavisani, O. Rezaifar, e A. Kheyroddin, «Multifunctional properties of shape memory materials in civil engineering applications: A state-of-the-art review», *JOBE,* vol. 44, p. 102657, dic. 2021. https://doi.org/10.1016/j.jobe.2021.102657

[6] M. C. Biswas, S. Chakraborty, A. Bhattacharjee, e Z. Mohammed, «4D Printing of Shape Memory Materials for Textiles: Mechanism, Mathematical Modeling, and Challenges», *Adv. Funct. Mater.*, vol. 31, fasc. 19, p. 2100257, 2021. https://doi.org/10.1002/adfm.202100257

[7] M. O. Gök, M. Z. Bilir, e B. H. Gürcüm, «Shape-Memory Applications in Textile Design», *Procedia Soc.*, vol. 195, pp. 2160–2169, lug. 2015. https://doi.org/10.1016/j.sbspro.2015.06.283

[8] M. Mehrpouya, A. Azizi, S. Janbaz, e A. Gisario, «Investigation on the Functionality of Thermoresponsive Origami Structures», *Adv. Funct. Mater.*, vol. 22, fasc. 8, p. 2000296, 2020. https://doi.org/10.1002/adem.202000296

[9] H. E. Karaca, E. Acar, H. Tobe, e S. M. Saghaian, «NiTiHf-based shape memory alloys», *Mater. Sci. Technol.*, vol. 30, fasc. 13, pp. 1530–1544, nov. 2014. https://doi.org/10.1179/1743284714Y.0000000598

[10] I. Akbar, M. El Hadrouz, M. El Mansori, e D. Lagoudas, «Toward enabling manufacturing paradigm of 4D printing of shape memory materials: Open literature review», *Eur. Polym. J.*, vol. 168, p. 111106, apr. 2022. https://doi.org/10.1016/j.eurpolymj.2022.111106

[11] A. Subash e B. Kandasubramanian, «4D printing of shape memory polymers», *Eur. Polym. J.*, vol. 134, p. 109771, lug. 2020. https://doi.org/10.1016/j.eurpolymj.2020.109771

[12] S. Joshi *et al.*, «4D printing of materials for the future: Opportunities and challenges», *Applied Materials Today*, vol. 18, p. 100490, mar. 2020. https://doi.org/10.1016/j.apmt.2019.100490

[13] E. Pei e G. H. Loh, «Technological considerations for 4D printing: an overview», *Prog Addit Manuf*, vol. 3, fasc. 1, pp. 95–107, giu. 2018. https://doi.org/10.1007/s40964-018-0047-1

[14] A. Alderson *et al.*, «Elastic constants of 3-, 4- and 6-connected chiral and anti-chiral honeycombs subject to uniaxial in-plane loading», *Compos Sci Technol*, vol. 70, fasc. 7, Art. fasc. 7, lug. 2010. https://doi.org/10.1016/j.compscitech.2009.07.009

[15] A. Sorrentino, D. Castagnetti, L. Mizzi, e A. Spaggiari, «Bio-inspired auxetic mechanical metamaterials evolved from rotating squares unit», *Mech. Mater.*, vol. 173, p. 104421, ott. 2022. https://doi.org/10.1016/j.mechmat.2022.104421

[16] A. Papadopoulou, J. Laucks, e S. Tibbits, «Auxetic materials in design and architecture», *Nat Rev Mater*, vol. 2, fasc. 12, Art. fasc. 12, dic. 2017. https://doi.org/10.1038/natrevmats.2017.78

[17] M. Mehrpouya, T. Edelijn, M. Ibrahim, A. Mohebshahedin, A. Gisario, e M. Barletta, «Functional Behavior and Energy Absorption Characteristics of Additively Manufactured Smart Sandwich Structures», *Adv. Eng. Mater.*, vol. 24, fasc. 9, Art. fasc. 9, 2022. https://doi.org/10.1002/adem.202200677

[18] T. Li, J. Sun, J. Leng, e Y. Liu, «Quasi-static compressive behavior and energy absorption of novel cellular structures with varying cross-section dimension», *Compos. Struct.*, vol. 306, p. 116582, feb. 2023. https://doi.org/10.1016/j.compstruct.2022.116582

[19] A. P. Valerga, M. Batista, J. Salguero, e F. Girot, «Influence of PLA Filament Conditions on Characteristics of FDM Parts», *Mater.*, vol. 11, fasc. 8, Art. fasc. 8, ago. 2018. https://doi.org/10.3390/ma11081322

[20] M. Barletta, A. Gisario, e M. Mehrpouya, «4D printing of shape memory polylactic acid (PLA) components: Investigating the role of the operational parameters in fused deposition modelling (FDM)», *JMP*, vol. 61, pp. 473–480, gen. 2021. https://doi.org/10.1016/j.jmapro.2020.11.036

[21] A. Forés-Garriga, G. Gómez-Gras, e M. A. Pérez, «Mechanical performance of additively manufactured lightweight cellular solids: Influence of cell pattern and relative density on the printing time and compression behavior», *Mater. Des.*, vol. 215, p. 110474, mar. 2022. https://doi.org/10.1016/j.matdes.2022.110474

[22] W. Zhang *et al.*, «Characterization of residual stress and deformation in additively manufactured ABS polymer and composite specimens», *Compos Sci Technol*, vol. 150, pp. 102–110, set. 2017. https://doi.org/10.1016/j.compscitech.2017.07.017

[23] L. J. Gibson, «Cellular Solids», *MRS Bulletin*, vol. 28, fasc. 4, Art. fasc. 4, apr. 2003. https://doi.org/10.1557/mrs2003.79

[24] A. Yousefi, S. Jolaiy, M. Lalegani Dezaki, A. Zolfagharian, A. Serjouei, e M. Bodaghi, «3D-Printed Soft and Hard Meta-Structures with Supreme Energy Absorption and Dissipation Capacities in Cyclic Loading Conditions», *Adv. Eng. Mater.*, p. 2201189, nov. 2022. https://doi.org/10.1002/adem.202201189